

Shell Model Embedded in the Continuum

K. Bennaceur^{1,2*}, N. Michel³, F. Nowacki⁴, J. Okołowicz^{3,5}, M. Płoszajczak³

¹ *Department of Physics and Astronomy, University of Tennessee, Knoxville, Tennessee 37996*

² *Physics Division, Oak Ridge National Laboratory, Oak Ridge, Tennessee 37831*

³ *Grand Accélérateur National d'Ions Lourds (GANIL), CEA/DSM - CNRS/IN2P3, BP 5027, F-14076 Caen cedex 05, France*

⁴ *Laboratoire de Physique Théorique, 3-5 rue de l'Université, F-67084 Strasbourg cedex, France*

⁵ *Institute of Nuclear Physics, Radzikowskiego 152, PL-31-342 Krakow, Poland*

The realistic shell model which includes coupling between the many-particle (quasi-)bound states and the continuum of one-particle scattering states provides the basic tool for a unified description of the structure of exotic nuclei and simple nuclear reactions involving exotic nuclei, like radiative capture reaction, Coulomb dissociation or elastic scattering. We discuss here some results concerning the nucleus of ^{17}F and the reactions $^{16}\text{O}(p, \gamma)^{17}\text{F}$ and $^{16}\text{O}(p, p)^{16}\text{O}$.

I. INTRODUCTION

A realistic description of exotic nuclei requires taking into account the coupling between discrete and continuum states which is responsible for unusual spatial features of these nuclei. Within the newly developed Shell Model Embedded in the Continuum (SMEC) approach [1], one may obtain a unified description of divergent characteristics of these states as well as the reactions involving one nucleon in the continuum. This aspect is particularly important in the studies near the drip lines where the amount of experimental information will be reduced, and one has to use structure and reaction data, both strongly limited, to understand the basic properties of these nuclei. On the other hand, unifying features of the SMEC approach provide a stringent test for the approximations involved in the calculations

The quality of the SMEC description depends crucially on the realistic account of the configuration mixing for the coexisting low-lying structures and hence on the quality of the Shell Model (SM) effective interaction and the SM space considered. In this article we shall discuss how this configuration influences the Coulomb dissociation (CD) and proton elastic scattering cross-section, providing a reliable measure of the structural properties.

II. THE MODEL

The SMEC is mainly based on the Continuum Shell Model [2], the main difference being in our treatment a more realistic description of the discrete levels, which is an essential condition for the study of low-lying excitations. In the SMEC formalism, the atomic nucleus is considered as an open quantum system, *i.e.* the sub-spaces \mathcal{Q} of (quasi-)bound states and \mathcal{P} of scattering states are not separated artificially. The \mathcal{P} sub-space contains the states with $N-1$ particles in bound orbits coupled to one particle that can occupy scattering states, while the \mathcal{Q} sub-space corresponds to the configurations where all particles occupy bound or quasi-bound levels. We only consider states with asymptotically at most one particle in the continuum, so the projectors P and Q on the sub-spaces fulfill the condition:

$$P + Q = 1. \quad (1)$$

Using the projection technique, we split the Schrödinger equation into three different ones, describing the system in each sub-space and the coupling between them. The key element of our treatment is the realistic description of the discrete levels. Using the code ANTOINE [3], we solve the standard Shell Model (SM) problem:

$$H_{QQ}\Phi_i = E_i\Phi_i, \quad (2)$$

where $H_{QQ} = QHQ$ is identified with a realistic SM Hamiltonian. The eigenstates Φ_i are the N -particle (quasi-)bound wave functions. We believe that for a quantitative description of the low-lying states in the exotic nuclei one has to

*karim@mail.phy.ornl.gov

use as a starting point the accurate many-body wave functions provided by the SM with effective interactions in order to generate some realistic *internal mixing* of the many-body wave functions in the \mathcal{Q} sub-space.

To generate the single particle wave functions in the \mathcal{Q} sub-space and the radial part of the scattering states in the \mathcal{P} sub-space, we use a finite depth potential of Woods-Saxon (WS) type with a spin-orbit and a Coulomb part:

$$U(r) = V_0 f(r) + V_{\text{SO}} \lambda_\pi^2 (2\mathbf{l} \cdot \mathbf{s}) \frac{1}{r} \frac{df(r)}{dr} + V_C, \quad (3)$$

where $\lambda_\pi^2 = 2 \text{ fm}^2$ is the pion Compton wavelength and $f(r)$ is the radial form factor: $f(r) = [1 + \exp((r - R_0)/a)]^{-1}$. The Coulomb part, V_C , is calculated for a uniformly charged sphere with radius R_0 . This potential is used to generate the single particle wave functions in the \mathcal{Q} sub-space. The single particle resonances are included using a cut-off technique, *i.e.* the resonance wave functions for $r < R_{\text{cut}}$ are included in \mathcal{Q} and normalized, while the exterior part is left in \mathcal{P} . The wave functions in \mathcal{P} and \mathcal{Q} are properly orthogonalized in order to ensure the orthogonality of the two sub-spaces. The potential (3) is modified due to the residual interaction through a self-consistent procedure. The single particle states used to build the \mathcal{Q} sub-space correspond actually to the modified (*i.e.* converged) potential. We choose the parameters in (3) so that the modified potential meets some conditions required by the system we want to study.

For the continuum states, we solve the coupled channel equations:

$$(E - H_{PP}) \xi_E^{c(+)} = \sum_{c'} (E - H_{cc'}) \xi_E^{c'(+)}, \quad (4)$$

where c denotes the different channels and $H_{PP} = PHP$. The superscript (+) means that boundary conditions for outgoing scattering states are used for $c' \neq c$. The solutions of these equations are the non-resonant part of the scattering states. The coupling between channels depends on the structure of the N and $N - 1$ particle systems and is determined microscopically. The third system of equations to be solved consists of the inhomogeneous coupled channel equations:

$$(E - H_{PP}) \omega_i^{(+)} = H_{PQ} \omega_i^{(+)} = w_i, \quad (5)$$

in which the source term is primarily given by the SM structure of the N -particle state Φ_i . The solution of this equation represents the continuation of the discrete state Φ_i in the \mathcal{P} sub-space and describes the fact that a discrete level can decay by emitting a nucleon. The asymptotic form of the function $\omega_i^{(+)}$ determines the position for the one-particle threshold. The reduced matrix element of the source term in equation (5), which involves two annihilation and one creation operator, $\mathcal{R}_{\gamma\delta(L)\beta}^{j\alpha} = [a_\beta^\dagger (\tilde{a}_\gamma \tilde{a}_\delta)^L]^{j\alpha}$, is computed between different initial states in the N -body system and final states in the system with $N - 1$ particles. Hence, the description of the coupling between the \mathcal{P} and \mathcal{Q} sub-spaces will strongly depend on the description of the structure of the N and $N - 1$ particle systems.

In equations (4) and (5), the residual coupling between channels ($\mathcal{P} - \mathcal{P}$) and between the two sub-spaces ($\mathcal{P} - \mathcal{Q}$) are modeled by a zero range force. This force will provide the *external mixing* of the SM configurations via the virtual excitations of particles to the continuum states.

The three distinct functions are then used to express the many-body scattering solutions of the problem and the discrete states wave functions modified by the coupling to the continuum:

$$\begin{aligned} \Psi_E^c &= \xi_E^c + \sum_{i,j} \Omega_i^{(+)} \frac{1}{E - H_{QQ}^{eff}} \langle \Phi_j | H_{QP} | \xi_E^c \rangle, \\ \Omega_i^{(+)} &= \Phi_i + \omega_i^{(+)}. \end{aligned} \quad (6)$$

The latter are related with the effective Hamiltonian:

$$H_{QQ}^{eff} = H_{QQ} + H_{QP} G_P^{(+)} H_{PQ}, \quad (7)$$

where $G_P^{(+)}$ is the Green function for the motion of single particles in the \mathcal{P} sub-space. This effective Hamiltonian has complex energy-dependent eigenvalues $E_i - i\Gamma_i/2$. These eigenvalues at energy $E_i(E) = E$ determine the energies and widths of the nuclear states.

As can be seen in equation (6), this formalism is fully symmetric and consistent in treating the continuum and discrete part of the solutions, the continuum states being modified by all the discrete states, and the discrete levels being modified by the coupling to the continuum.

III. APPLICATIONS

The SMEC wave function can be used to calculate various observables such as excitation spectra, static nuclear moments, and nuclear radii, as well as cross-sections for radiative capture, Coulomb dissociation, or elastic scattering. In the description of ^{17}F it is important to take into account the dynamics of the ^{16}O core and to include the $2p-2h$ and $4p-4h$ excitations from p -shell to sd -shell. The ZBM effective SM interaction [4] in the SM space corresponding to the $0p_{1/2}$, $0d_{5/2}$ and $1s_{1/2}$ orbitals allows for taking correctly into account these dynamics. The valence space ($0p_{1/2}, 0d_{5/2}, 1s_{1/2}$) has the advantage of being practically non-spurious. Moreover, most of the states at the $p-sd$ interface are well described through the configuration mixing of these three orbitals.

The parameters of the potential (3) have been adjusted in order that the single particle energies of the $0d_{5/2}$, $1s_{1/2}$, and $0d_{3/2}$ in the modified potential are equal to the energies of the $5/2_1^+$, $1/2_1^+$, and $3/2_1^+$ many-body states respectively. For the residual interaction between the \mathcal{P} and \mathcal{Q} sub-spaces, we have used the DDSM1 interaction [5]:

$$V_{12} = \left[\rho(r) \hat{v}_{00}^{in} + (1 - \rho(r)) \hat{v}_{00}^{ex} + \tau_1 \cdot \tau_2 \left(\rho(r) \hat{v}_{01}^{in} + (1 - \rho(r)) \hat{v}_{01}^{ex} \right) \right] \delta(\vec{r}_1 - \vec{r}_2), \quad (8)$$

where $\rho(r) = [1 + \exp((r - r_0)/d)]^{-1}$, with $r_0 = 2.64$ fm and $d = 0.58$ fm. The DDSM1 interaction has four parameters: $v_{00}^{in} = 36.45$, $v_{00}^{ex} = -297.9$, $v_{01}^{in} = 109.4$ and $v_{01}^{ex} = 115.5$, all given in $\text{MeV}\cdot\text{fm}^3$.

A. The structure of ^{17}F

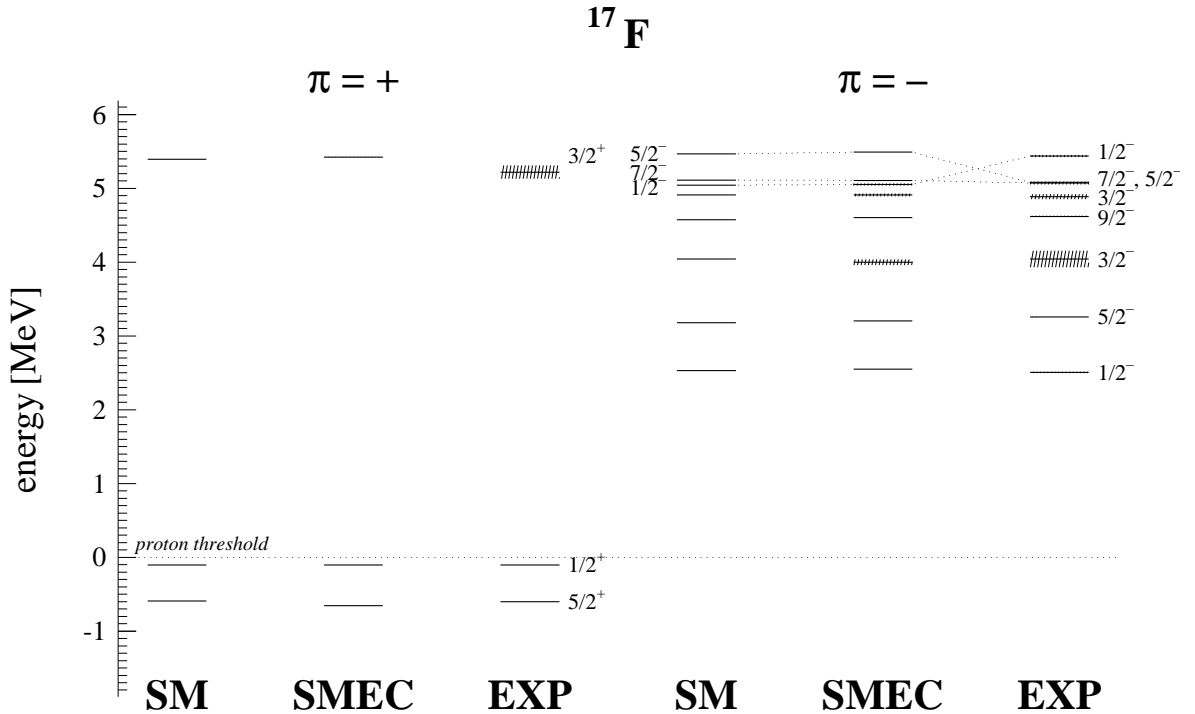


FIG. 1. SM and SMEC energy spectra obtained with the ZBM effective SM interaction [4] are compared with the experimental states of the ^{17}F nucleus. The DDSM1 [5] interaction is used for the residual coupling between \mathcal{P} and \mathcal{Q} . The proton threshold energy is adjusted to reproduce the position of the first $1/2^+$ state. The shaded regions represent the width of the resonances.

It has been shown in a previous study [5] that a correct reproduction of the properties ^{17}F requires an accurate description of both the internal and external mixing. This requirement cannot be fulfilled in the $p-sd$ SM space if we consider only the $1p-0h$ and $2p-1h$ configurations for the positive and negative parity states, respectively. This observation has motivated the use of the ZBM effective interaction in the $(0p_{1/2}, 0d_{5/2}, 1s_{1/2})$ model space, for which the internal mixing is realistically described.

In figure 1, we show the results for the energies and width obtained in the SMEC approach, compared with the SM results and the experimental data. The energy of the proton threshold has been adjusted in order to reproduce accurately the energy of the excited state $1/2_1^+$, this condition being required to reproduce correctly the low-energy part of the proton capture by ^{16}O . The $3/2_1^+$ state at 4400 MeV cannot be reproduced in the considered SM space and is not represented on the figure.

B. Radiative capture reaction $^{16}\text{O}(p, \gamma)^{17}\text{F}$ and Coulomb dissociation of ^{17}F

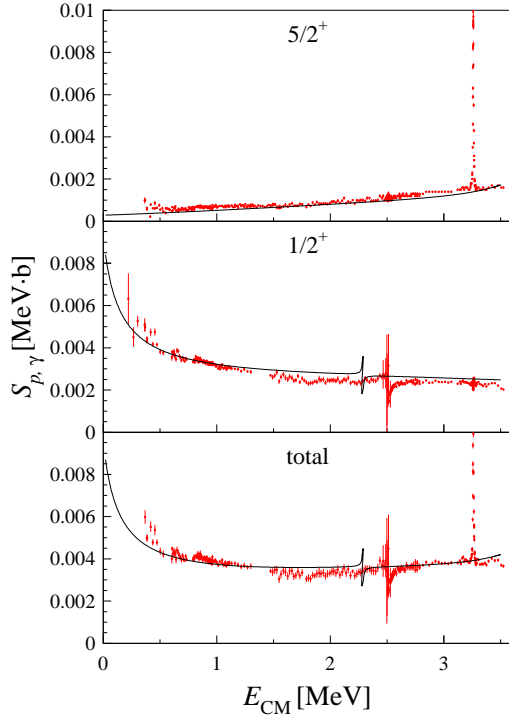


FIG. 2. The astrophysical factor $S_{p\gamma}$ for the reactions $^{16}\text{O}(p, \gamma)^{17}\text{F}(J^\pi = 5/2_1^+)$ and $^{16}\text{O}(p, \gamma)^{17}\text{F}(J^\pi = 1/2_1^+)$ is plotted as a function of the center of mass energy E_{CM} . The experimental points are taken from [6]. The contribution from the $5/2_1^-$ resonance in the $^{16}\text{O}(p, \gamma)^{17}\text{F}(J^\pi = 5/2_1^+)$ branch is very narrow and has been omitted in the figure. The resonance is found at 3.29 MeV in the SMEC-DDSM1 calculations.

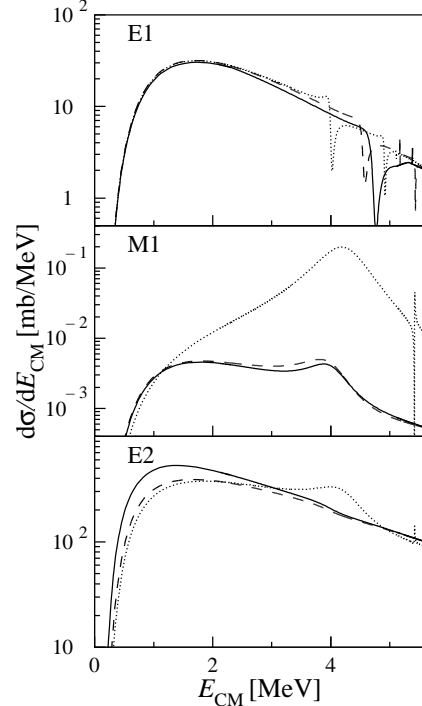


FIG. 3. The Coulomb dissociation cross section for the break-up of ^{17}F on a ^{208}Pb target at 10 MeV.A is plotted as a function of the $p - ^{17}\text{F}$ center of mass energy separately for $E1$, $M1$, and $E2$ components. The solid and dashed lines represent the calculation using the psd SM interaction. The residual coupling is given either by a Wigner-Bartlett force with a spin-exchange parameter $\alpha = 0.27$ [1] (solid line) or by the DDSM1 interaction. The dotted line shows the results in the ZBM space with the DDSM1 residual coupling.

Using the first order perturbation theory, we have computed the cross-section and astrophysical S -factor for the reaction $^{16}\text{O}(p, \gamma)^{17}\text{F}(J^\pi)$. In figure 2 the calculated total astrophysical S -factor as a function of the center of mass energy, as well as its values for the $^{16}\text{O}(p, \gamma)^{17}\text{F}(J^\pi = 5/2_1^+)$ and $^{16}\text{O}(p, \gamma)^{17}\text{F}(J^\pi = 1/2_1^+)$ branches are compared with the experimental data [6]. We have taken into account all possible $E1$, $M1$, and $E2$ transitions from the incoming s , p , d , f , and g partial waves but only the $E1$ coming from the p waves gives an important contribution in the range of energy considered here. The energy dependence of the S -factor as $E_{\text{CM}} \rightarrow 0$ can be fitted by a second order polynomial to the point obtained in the interval from 20 KeV to 50 MeV. We have obtained $S(0) = 9.32 \times 10^{-3}$ MeV.b, and the logarithmic derivative $S'(0)/S(0) = -4.86$ MeV $^{-1}$.

The double differential cross-section for the Coulomb dissociation of ^{17}F from its ground state to the continuum with a definite multipolarity $\pi\lambda$ is given by:

$$\frac{d^2\sigma}{d\Omega_{17\text{F}^*}dE_{\text{CM}}} = \sum_{\pi\lambda} \frac{1}{E_{\text{CM}}} \frac{dn_{\pi\lambda}}{d\Omega_{17\text{F}^*}} \sigma_{\gamma}^{\pi\lambda}(E_{\gamma}), \quad (9)$$

where $\Omega_{17\text{F}^*}$ defines the direction of the center of mass of the $[^{16}\text{O} + p]$ system with respect to the beam direction. $\sigma_{\gamma}^{\pi\lambda}$ is the cross-section for the photo-disintegration process $\gamma + ^{17}\text{F} \rightarrow ^{16}\text{O} + p$, with photon energy E_{γ} and multipolarity $\pi = E$ (electric) or M (magnetic), and $\lambda=1, 2, \dots$ (order), which is related to that of the radiative capture process through the theorem of detailed balance. E_{γ} is given by $E_{\text{CM}} = E_{\gamma} + Q$, with $Q = 0.6$ MeV. In most cases, only one or two multipoles dominate the radiative capture and the Coulomb dissociation processes. In eq. (9), $n_{\pi\lambda}$ represents the number of virtual (equivalent) photons provided by the Coulomb field of the target [7].

The results for different SM effective interactions (ZBM or *psd* [5]) and different residual coupling (DDSM1 or the density-independent Wigner-Bartlett (WB) force [1]) are shown in figure 3. For all these different SM effective interactions and $Q - \mathcal{P}$ residual coupling, the proton capture is well reproduced.

The results for the $M1$ multipolarity strongly depend on the SM effective interaction (dotted and dashed line in the middle part of figure 3), but its contribution to the total CD is unimportant at these energies. No significant sensitivity to the residual $Q - \mathcal{P}$ coupling is seen in this cross-section. A strong sensitivity to the $Q - \mathcal{P}$ coupling is seen in the $E2$ multipolarity (lower part in figure 3). The calculation for the *psd* effective interaction using either DDSM1 (dashed line) or WB (solid line) residual coupling show a strong difference for the $E2$ cross-section. On the contrary, for the same DDSM1 residual coupling, there is a little dependence on the ground state correlations below $E_{\text{CM}} = 4$ MeV. Hence, the experimental resolution of the $E2$ and $M1$ contributions to the CD cross-section, together with the constraint provided by the experimentally well-known capture cross-section, provide a stringent test on the internal and external mixing in the SMEC wave function for the nuclei of ^{17}F .

C. Elastic scattering $^{16}\text{O}(p,p)^{16}\text{O}$

Figure 4 compares the calculated elastic excitation function at a laboratory angle $\theta = 166^{\circ}$ with experimental data [8]. In the upper part, the calculations are performed using the *psd* SM effective interaction [5] with (solid line) or without (dashed line) the contribution from the $5/2_1^+$ state to the cross-section. In this calculation, only the $0\hbar\omega$ configurations are considered for the natural parity states, and $1\hbar\omega$ for the non-natural ones. Hence, in order to take into account for the effect of the higher order correlations, the matrix elements of the coupling between \mathcal{P} and \mathcal{Q} had to be quenched [5]. This quenching prescription allows for reproducing correctly the spectrum of ^{17}F and the radiative capture cross-section of protons by ^{16}O but fails to reproduce the elastic scattering data. This can notably be seen at low energy where the computed cross section is about 25 % smaller than the experimental value. It turns out that the diminution of the cross section at low energy is due to the strong resonant contribution from the $5/2_1^+$ state. By artificially removing this contribution, the low energy part of the cross-section gets closer to the experimental data (dashed line). This suggests that the real source of this anomaly in the proton elastic cross-section is the non-locality of the effective Hamiltonian (7) in \mathcal{Q} sub-space for positive energies. This non locality is caused by virtual coupling of discrete and continuum states. For the energies below the proton threshold, the coupling to the continuum introduces a hermitian modification to the Hamiltonian $H_{\mathcal{Q}\mathcal{Q}}$ which shifts the energy of the $5/2_1^+$ state. For excitation energies above the proton threshold, the coupling between \mathcal{P} and \mathcal{Q} generates a non-hermitian correction which yields the imaginary part of the eigenvalues of $H_{\mathcal{Q}\mathcal{Q}}^{\text{eff}}$ and, hence, produce the resonant behaviour. The internal mixing of configurations in the \mathcal{Q} sub-space tends to reduce this resonant behaviour for the positive energies, which, in general is strongest for the states having a small internal mixing.

A more correct picture of configuration mixing is expected in the ZBM model space. The lower part of figure 4 compares the elastic excitation function in this approximation with the experimental data [8]. Indeed, the agreement of the SMEC results, taking correctly into account the dynamics of the ^{16}O core with the experimental data, is very good in almost the entire energy range covered by the experimental data. This example shows that whenever the ground state of a studied $N - 1$ particle system is highly correlated, *i.e.* whenever the contribution of $0p-0h$ correlations is reduced and higher order correlations predominate, one may expect a strong reduction of the non-hermitian correction for positive energies from the bound state of the N particle system.

IV. CONCLUSION

We have shown in this work that the realistic SM extended to include the coupling to the continuum is a powerful tool, not only for the study of exotic nuclei, but also for the reaction data involving one nucleon in the continuum. The cornerstone of this model is the effective SM interaction providing a realistic internal mixing of configurations in the \mathcal{Q} sub-space. In the SMEC approach, one may use different observables to fix the few parameters such as the strength of the residual $Q - \mathcal{P}$ coupling or the radius and depth of the initial average potential. Moreover, the information about the amount of correlations in the low-lying coexisting states can be extracted not only from the

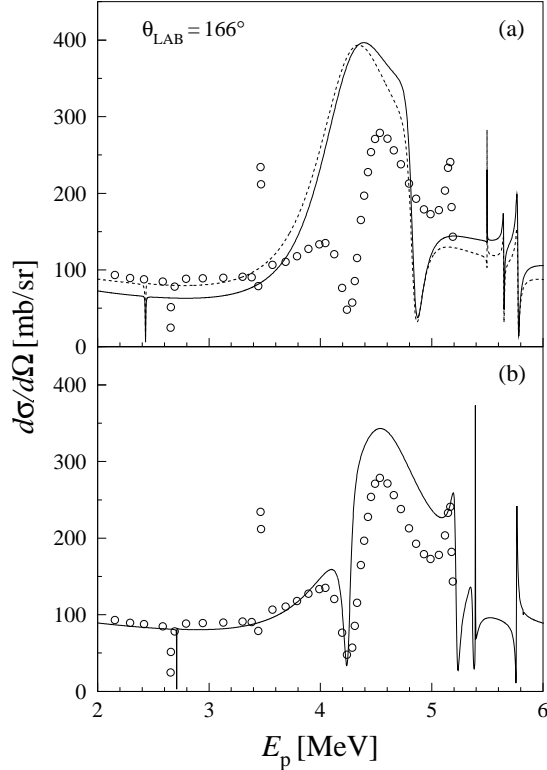


FIG. 4. The elastic cross-section at laboratory angle $\theta_{\text{LAB}} = 166^\circ$ for the $p + {}^{16}\text{O}$ scattering as a function of the proton energy E_p . The SMEC calculations have been performed in the ZBM model space (lower part) or using the psd effective SM interaction (upper part). In both cases, the coupling between the \mathcal{P} and \mathcal{Q} sub-spaces is given by the DDSM1 residual interaction. The results shown with the dashed line (upper part) do not include the resonant contribution from the $5/2_1^+$ state. Experimental cross sections are from [8].

spectroscopic data, but also from the elastic excitation function. For nuclei far from stability, where the amount of experimental data is strongly limited, this feature of the model is very attractive.

ACKNOWLEDGMENTS

The authors want to thank Professor R. Shyam for numerous discussions during the development of this work. This research was partly supported by the U.S. Department of Energy under contracts DE-FG02-96ER40963 (University of Tennessee) and DE-AC05-00OR22725 (ORNL).

-
- [1] K. Bennaceur *et al.*, J. Phys. **G 24**, 1631 (1998); Nucl. Phys. **A 651**, 289 (1999).
 - [2] H. W. Barz, I. Rotter and J. Höhn, Nucl. Phys. **A 275**, 111 (1977).
 - [3] E. Caurier, code ANTOINE (unpublished).
 - [4] A.P. Zuker, B. Buck and J.B. McGrory, Phys. Rev. Lett. **21**, 39 (1968).
 - [5] K. Bennaceur *et al.*, Nucl. Phys. **A 671**, 203 (2000); Phys. Lett. **B 488**, 75 (2000).
 - [6] R. Morlock *et al.*, Phys. Rev. Lett. **79**, 3837 (1997).
 - [7] A.N.F. Alexio and C.A. Bertulani, Nucl. Phys. **A 505**, 448 (1989).
 - [8] S.R. Salisbury *et al.*, Phys. Rev. **126**, 2143 (1962).